

Protective effect of hydroxysafflor yellow A on renal ischemia-reperfusion injury by targeting the Akt-Nrf2 axis in mice

YUEMING WANG^{1*}, KAIYUE HAN^{2*}, ZILE LI², XIAOXUAN TANG², CHEN WANG², YAXUAN ZHAO², HENGCHAO ZHANG², ZIRAN GENG², JIE KONG², XIYING LUAN² and YANLIAN XIONG³

Departments of ¹Pathogen Biology, ²Immunology and ³Anatomy, School of Basic Medicine, Binzhou Medical University, Yantai 264003, P.R. China

Received September 13, 2022; Accepted October 14, 2022

DOI: 10.3892/etm.2022.11677

Abstract. Ischemic/reperfusion (I/R) injury is the primary cause of acute kidney injury (AKI). Hydroxysafflor yellow A (HSYA), a natural compound isolated from *Carthamus tinctorius* L., has been found to possess anti-inflammatory and antioxidant properties. However, the protective effects and potential mechanism of HSYA on I/R-induced AKI remains unclear. In the present study, the *in vitro* hypoxia/reoxygenation (H/R) and *in vivo* renal I/R models were employed to investigate the renal protective effects and molecular mechanisms of HSYA on I/R-induced AKI. The present results indicated that HSYA pretreatment significantly ameliorated renal damage and dysfunction in the I/R injury mice via enhancing the antioxidant capacity and suppressing the oxidative stress injury, inflammatory response, and apoptosis. Mechanistic studies showed that HSYA could upregulate Akt/GSK-3 β /Fyn-Nrf2 axis-mediated antioxidant gene expression both *in vitro* and *in vivo*. Moreover, HSYA-mediated improvement in antioxidant, anti-inflammatory, and anti-apoptotic effects in H/R-treated HK-2 cells was abrogated by Akt inhibitor LY294002 supplementation. In summary, the present results demonstrated that HSYA attenuated kidney oxidative stress, inflammation response, and apoptosis induced by I/R, at least in part, via activating the Akt/GSK-3 β /Fyn-Nrf2 axis pathway. These findings provided evidence that HSYA may be applied as a potential therapeutic agent in the treatment of I/R induced AKI.

Introduction

Ischemia-reperfusion (I/R) injury is a major cause of acute kidney injury (AKI), which has a high morbidity and mortality rate (1). It was found that AKI was accompanied by free radical burst, which promoted inflammatory response and apoptosis in the kidney (2). Herein, effective antioxidants against reactive oxygen species (ROS) stress may be applied to protect against I/R-induced renal injury and dysfunction.

It has been reported that AKI is accompanied by the imbalance between oxidation and antioxidation metabolism in renal tissue, which is manifested by the outbreak of free radicals and the increase of oxidative stress (3). And further lead to the increase of inflammatory response, DNA damage, and endoplasmic reticulum stress, and finally induce renal cell apoptosis (4,5). Nuclear factor erythroid 2-related factor 2 (Nrf2) is considered a key regulator for maintaining the redox balance and is involved in the initiation of the transcriptional expression of downstream antioxidant enzymes (6). According to recent studies, Nrf2 activation plays a pivotal role in preventing I/R induced multiple organ injury by upregulating antioxidant, anti-inflammatory, and anti-apoptotic effects (3,7-9).

Hydroxysafflor yellow A (HSYA, molecular formula, C₂₇H₃₂O₁₆; molecular weight, 612.53 g/mol), derived from *Carthamus tinctorius* L. (Fig. 1A and B), is a chalcone glycoside and predominantly used for therapy against multiple organ injury dependent on its antioxidant, anti-inflammatory, and anti-apoptotic properties (10). Previous studies suggested that HSYA may protect the myocardium, cerebral, liver, and kidney from I/R injury (11-14). According to previous studies, administration with HSYA ameliorates I/R induced AKI via blockade of TLR4/NF- κ B pathway (15). Additionally, studies showed that HSYA played protective effects against myocardial I/R injury by activating the Akt/Nrf2/HO-1 pathway (16). However, whether HSYA protects against I/R induced AKI via Nrf2-mediated exogenous antioxidant defenses and its influence on AKI-related renal dysfunction remain to be elucidated.

The purpose of the present study was to evaluate the protective effects and underlying mechanisms of HSYA against renal I/R injury in both *in vitro* and *in vivo* models. The present results showed that HSYA could be used for preventing I/R-induced renal injury via targeting the Akt/GSK-3 β /Fyn-Nrf2 axis pathway.

Correspondence to: Professor Xiyang Luan or Professor Yanlian Xiong, Department of Immunology, School of Basic Medicine, Binzhou Medical University, 346 Guanhai Road, Yantai, Shandong 264003, P.R. China
E-mail: xiyang_luan@163.com
E-mail: xyl8807@163.com

*Contributed equally

Key words: ischemic/reperfusion, acute kidney injury, hydroxysafflor yellow A, nuclear factor erythroid 2-related factor 2

Materials and methods

Animals and ethics statement. Male C57BL/6 mice (8 weeks old, 20–24 g) were obtained from the animal research center at Luye Pharmaceutical Co., Ltd. (Shandong, China; SYXK 2018-0028). Mice were housed in a standard environment (40–60% humidity and 25°C temperature) with a regular light/dark cycle and free access to water and chow diet. The project was approved (approval no. 2021-11) by the Ethics Committee of Binzhou Medical University (Yantai, China).

Establishment of the renal I/R model. The mice model of renal I/R injury was induced according to the protocol previously described (17). Mice were fully anesthetized with pentobarbital sodium (50 mg/kg, i.p.) and placed on a homeothermic table to maintain core body temperature at 37°C. A midline laparotomy was then performed in which the abdominal cavity was fully exposed. Next, the left kidney was subjected to 30 min of ischemia with a non-traumatic vascular clamp followed by reperfusion.

The mice were randomly and equally divided into 3 groups (n=10) as depicted in Fig. 1C: Sham group, the right kidney was extirpated for sham-operated animals, but neither clamping nor infusion was performed in the left kidney; HSYA group, mice subjected to renal I/R injury were treated with HSYA (100 mg/kg/day) by intraperitoneal injection for 7 consecutive days before the I/R model established; I/R group, mice subjected to renal I/R injury were treated with an identical volume of saline as the vehicle. HSYA (purity >98%) was purchased from MedChemExpress (cat. no. HY-N0567). Analgesics (carprofen, 5 mg/kg, s.c.) and anaesthetics (propofol, 26 mg/kg, i.v.) were used to minimize the suffering of mice during the surgery. A total of 24 h after the I/R procedure, mice were anesthetized with pentobarbital sodium (40 mg/kg, i.p.) and blood was collected from the eye socket, then sacrificed by cervical dislocation. After careful evaluation, an animal would be sacrificed if it began to exhibit symptoms of hypothermia (colonic temperature of 34°C) or weight loss >20% (the maximum percentage of body weight loss observed in the present study was 21.3%), including hunched posture, immobility, ruffled fur, failure to eat, and failure to drink. The animal would be sacrificed right away to minimize pain if it was unable to stand, had trouble breathing, had significant muscle tightness, severe ulceration, or bled heavily. Twice daily, special crew monitored and recorded the health and behavior of the animals (once in the morning and once in the evening). C57BL/6 mice (n=30) were euthanized after the experiment. Mice were confirmed dead when there was no autonomous respiration and no reflex activity, and no heart activity. The kidneys were harvested, some of them were fixed in 4% paraformaldehyde for histological evaluation, and the others were snap-frozen in liquid nitrogen and stored at -80°C for subsequent protein and mRNA analysis.

Assessment of kidney functions. Blood was received immediately after the mice were sacrificed. The blood was centrifuged at 3,000 x g for 15 min at 4°C to collect serum. Concentrations of blood urea nitrogen (BUN; cat. no. C013-2-1) and serum creatinine (SCr; cat. no. C011-2-1) were measured using assay kits (Nanjing Jiancheng Bioengineering Institute).

Histology and immunohistochemistry. Kidney tissues were fixed with 4% formaldehyde for 24 h at 4°C and embedded in paraffin, and then cut into 4-μm sections and taken on slides. The prepared slides were deparaffinized twice in xylene and rehydrated in gradient ethanol, and then stained separately with Hematoxylin and Eosin (H&E) (5 min each, room temperature). Tissue damage was assessed in a blinded manner and scored using a tubular damage score as previously described (18), these changes included tubular epithelial cell swelling, vacuolization, cast formation, and desquamation. The specimens were analyzed by confocal microscopy (FV1000; Olympus Corp.).

Detection of oxidative stress. RIPA lysis buffer (1 ml; cat. no. R0010; Beijing Solarbio Science & Technology Co., Ltd.) was added to 100 mg of renal tissue and homogenized with glass homogenizer. It was then placed on ice for 30 min to render it fully homogenized, and then centrifuged at 13,000 x g for 15 min at 4°C, and finally supernatants were collected. ELISA was used to detect 8-hydroxyguanosine (8-OH-dG; cat. no. STA-320-T; Cell BioLabs, Inc.) in renal tissue, and the colorimetric method was used to detect malondialdehyde (MDA; cat. no. S0131S) and ROS (cat. no. S0033S; both from Beyotime Institute of Biotechnology) levels in renal tissue by using Multiskan FC Microplate Reader (Thermo Fisher Scientific, Inc.) and Orion AquaMate UV-Vis spectrophotometer (Thermo Fisher Scientific, Inc.) referring to the product manual for specific determination methods. The manufacturer's instructions for the corresponding assay kit were followed.

Detection of antioxidant capacity. The homogenized renal tissue was collected according to the aforementioned method, and the amine oxidase copper containing (T-AOC; cat. no. A015-1-2), superoxide dismutase (SOD; cat. no. A001-3-2), and catalase (CAT; cat. no. A007-1-1) activities of kidney tissue were measured by the Orion AquaMate UV-Vis spectrophotometer (Thermo Fisher Scientific, Inc.) with commercial kits (all from Nanjing Jiancheng Bioengineering Institute). The manufacturer's instructions for the corresponding assay kit were followed. Briefly, the protein concentration of the tissue and cells were first detected by using a Bradford Protein Assay kit (cat. no. P0006; Beyotime Institute of Biotechnology), then the commercial kit was used to detect the enzyme activity of the unit volume sample and calculate the enzyme activity under the same protein concentration. For example, the detection formula of SOD enzyme activity is as follows: SOD activity (U/mg protein) = [OD (control group) - OD (test group)] / [OD (control group)] ÷ 50% x [(Total volume) / (Sample volume)] ÷ Protein concentration (mg prot/ml).

Detection of proinflammatory cytokines. The serum inflammatory cytokines including monocyte chemoattractant protein-1 (MCP-1), tumor necrosis factor-α (TNF-α), and interleukin-1β (IL-1β) were measured by the Multiskan FC Microplate Reader (Thermo Fisher Scientific, Inc.). MCP-1 (cat. no. SEKP-0019), TNF-α (cat. no. SEKM-0034), and IL-1β (cat. no. SEKM-0002) ELISA kits were obtained all from Beijing Solarbio Science & Technology Co., Ltd. The manufacturer's instructions for the corresponding assay kit were followed.

RNA extraction and reverse transcription-quantitative (RT-q) PCR. Total RNA was extracted from kidney tissue using Trizol® Reagent (Invitrogen; Thermo Fisher Scientific, Inc.) following the manufacturer's instructions. The concentration of total RNA was detected using a biological spectrometer (NanoDrop 2000; Thermo Fisher Scientific, Inc.). A total of 1 µg of total RNA was reverse transcribed into cDNA at 37°C for 60 min and 4°C for 5 min using a First-strand cDNA Synthesis kit (cat. no. E6300L; New England BioLabs, Inc.) according to the manufacturer's protocol. qPCR assay was performed by using SYBR green dye on Step One sequence detection system (Applied Biosystems; Thermo Fisher Scientific, Inc.). The qPCR reaction conditions were subjected to an initial predenaturation step at 95°C for 3 min, followed by 39 cycles of 95°C for 20 sec and 60°C for 30 sec. Using β-actin as internal control, the relative abundance of genes was calculated using the $2^{-\Delta\Delta C_q}$ formula (19). Primer sequences are presented in Table SI.

Western blot analysis. The total protein was extracted from the kidney tissues and HK-2 cells. Briefly, 100 mg of kidney tissues or 5×10^5 HK-2 cells were homogenized in RIPA buffer for 10 min followed by centrifugation at $13,000 \times g$ for 10 min at 4°C. Nuclear proteins were extracted by a nuclear extraction kit (cat. no. ab113474; Abcam). The concentrations were detected by using a Bradford Protein Assay kit (cat. no. P0006; Beyotime Institute of Biotechnology). Western blot analyses were performed as previously described (20). Briefly, sodium dodecyl sulfate-polyacrylamide gel electrophoresis (SDS-PAGE) was performed by heating the samples for 8 min at 100°C and loading 10 µg membrane proteins on to a 5-15% linear acrylamide gradient gel (10 µg protein/lane). After blocked in 5% BSA (cat. no. SW3015; Beijing Solarbio Science & Technology Co., Ltd.) dissolved in TBS-20% Tween 20 (TBST) for 2 h at room temperature, PVDF membranes were then treated overnight at 4°C with primary antibodies against Nrf2 (1:3,000; cat. no. 12721), phosphorylated (p)-Akt (1:3,000; cat. no. 4060), Akt (1:3,000; cat. no. 9272), HO-1 (1:3,000; cat. no. 43966), NQO1 (1:3,000; cat. no. 62262), GSK-3β (1:3,000; cat. no. 12456), p-GSK-3β (1:3,000; cat. no. 5558), Fyn (1:3,000; cat. no. 4023), Histone H3 (1:3,000; cat. no. 4499), Cleaved Caspase-3 (1:3,000; cat. no. 9661) and GAPDH (1:3,000; cat. no. 5174) which were all obtained from Cell Signaling Technology, Inc. The membranes were then incubated with a secondary antibody (1:5,000; anti-rabbit IgG (H + L), cat. no. 14708; Cell Signaling Technology, Inc.) for 2 h at room temperature, followed by TBST washes. ECL plus detection reagents (cat. no. P0018FS; Beyotime Institute of Biotechnology) were used to visualize protein bands. The ImageJ gel analysis software (version 1.53; National Institutes of Health) was used for densitometric analysis.

Cell culture and hypoxia/reoxygenation (H/R) model. The human renal proximal tubular epithelial cell line (HK-2) was obtained from the Type Culture Collection of the Chinese Academy of Sciences and cultured at 37°C in DMEM/F-12 with 1% v/v penicillin/streptomycin and 10% v/v fetal bovine serum (cat. no. 10100147; Thermo Fisher Scientific, Inc.). A cell H/R model was established according to the previously described methods (21,22). Briefly, HK-2 cells were cultured for 12 h under hypoxic conditions (1% O₂, 5% CO₂, and 94% N₂)

in a medium without nutrients (glucose-free, serum-free) to induce hypoxic injury. Then, the medium was refreshed again, and the plates were moved to a normoxic cell incubator (5% CO₂ and 95% air) for 2 h. Control cells were incubated in a complete culture medium in a regular incubator (5% CO₂ and 95% air).

Cells were divided into five groups and were cultured with corresponding medium supplied with different reagents. The five groups included: i) Control group; ii) H/R model group; iii) H/R model + HSYA (5 µg/ml) group, HK-2 cells were pretreated with 5 µg/ml HSYA for 12 h; iv) H/R model + HSYA (10 µg/ml) group, HK-2 cells were pretreated with 10 µg/ml HSYA for 12 h; 5) H/R model + HSYA (20 µg/ml) group, HK-2 cells were pretreated with 20 µg/ml HSYA for 12 h; 6) H/R model + HSYA (20 µg/ml) group + Akt inhibitor LY294002 (30 µM) group, HK-2 cells were pretreated with 20 µg/ml HSYA and 30 µM LY294002 (cat. no. HY-10108; MedChemExpress) for 12 h.

Cell viability assay. Cell viability was assayed using CCK-8 (cat. no. C0037; Beyotime Institute of Biotechnology) according to the manufacturer's protocol. Briefly, HK-2 cells were cultured in six-well plates at a density of 5×10^4 /well. A total of 10 µl CCK-8 solution/well was added and HK-2 cells were incubated for 30 min at 37°C. The amount of formazan dye generated by cellular dehydrogenase activity was measured by absorbance at 450 nm with a microplate reader.

Statistical analysis. Statistical analyses were performed using SPSS (version 19.0; IBM Corp.). Three independent experiments are represented as the mean ± standard deviation. One way analysis of variance with Tukey's post hoc test and the unpaired Student's t-test were used for comparisons between groups. P<0.05 was considered to indicate a statistically significant difference.

Results

HSYA alleviates renal function parameters and histopathology in I/R mice. To determine the effect of HSYA on renal function after I/R, the concentration of SCr and BUN were evaluated. As shown in Fig. 1D and E, the concentration of SCr and BUN was significantly higher in the I/R group compared with the Sham group. However, compared with the I/R group, SCr and BUN concentrations were significantly decreased in the HSYA group.

To determine the effect of HSYA on renal injury after I/R, H&E staining renal histology were evaluated (Fig. 1F). H&E staining results revealed renal structural damage, inflammatory cell infiltration, and extracellular matrix deposition. However, pretreatment with HSYA reduced the severity of the tubular injury. Quantitative analysis showed that mice pre-treated with HSYA exhibited a significantly lower renal tubular damage score (Fig. 1G). These results indicated that HSYA ameliorated renal damage in the I/R mice.

HSYA exerts antioxidant effect on the kidney of I/R mice. To evaluate the antioxidant effect of HSYA on the kidney of I/R mice, the levels of oxidative stress and antioxidant biomarkers were analyzed. As revealed in Fig. 2A-C, the

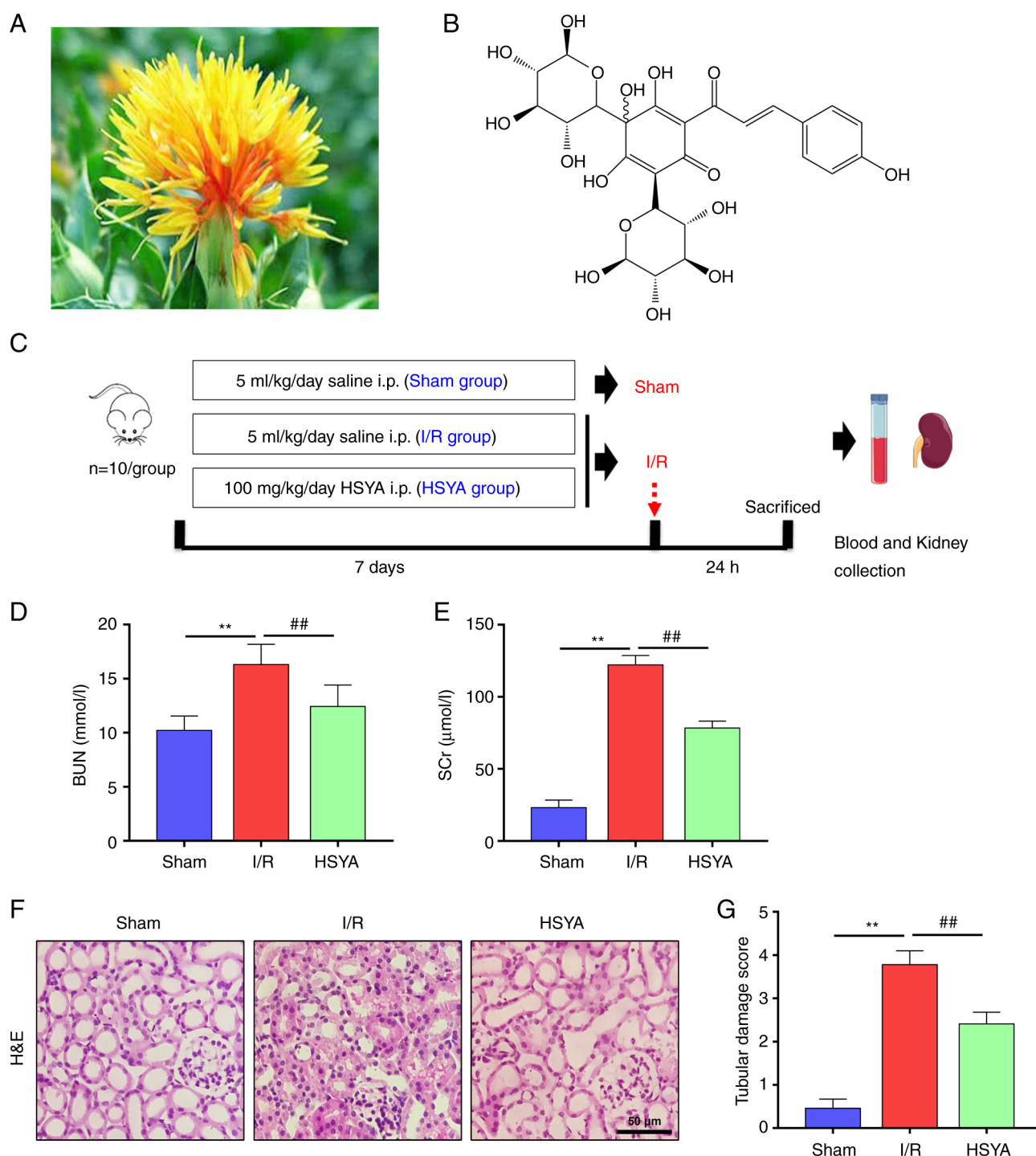


Figure 1. Effect of HSYA on renal function parameters and histopathology in the kidney of I/R mice. (A) The picture of *Carthamus tinctorius* L. (safflower). (B) The chemical structure of HSYA (molecular formula, C₂₇H₃₂O₁₆). (C) The scheme of the experimental design. Renal functions were assessed by (D) BUN and (E) SCr levels at the corresponding time points after I/R. (F) Representative photomicrographs of H&E stained kidney sections (scale bar, 50 μm). (G) Quantification of histological renal damage. All data are expressed as the mean ± SD. **P<0.01, Sham group vs. I/R group; ##P<0.01, I/R group vs. HSYA group. This image was produced using images from Servier Medical Art, licensed under a Creative Common Attribution 3.0 Generic License <http://smart.servier.com>. HSYA, Hydroxysafflower yellow A; BUN, blood urea nitrogen; SCr, serum creatinine; I/R, ischemia/reperfusion; H&E, hematoxylin and eosin.

activities of T-AOC, SOD, and CAT significantly decreased in the I/R group compared with the Sham group. Furthermore, pretreatment with HSYA significantly increased the activities of T-AOC, SOD, and CAT in comparison with the I/R group. By contrast, the levels of ROS, MDA, and 8-OH-dG significantly increased in the I/R group compared with the Sham group (Fig. 2D-F). Conversely, HSYA pretreatment

significantly decreased the levels of ROS, MDA, and 8-OH-dG in the kidney of I/R mice. These results indicated that HSYA treatment alleviates the imbalance of redox metabolic in the kidney of I/R mice.

HSYA ameliorates the expression of proinflammatory cytokines in I/R mice. The effect of HSYA on the expression

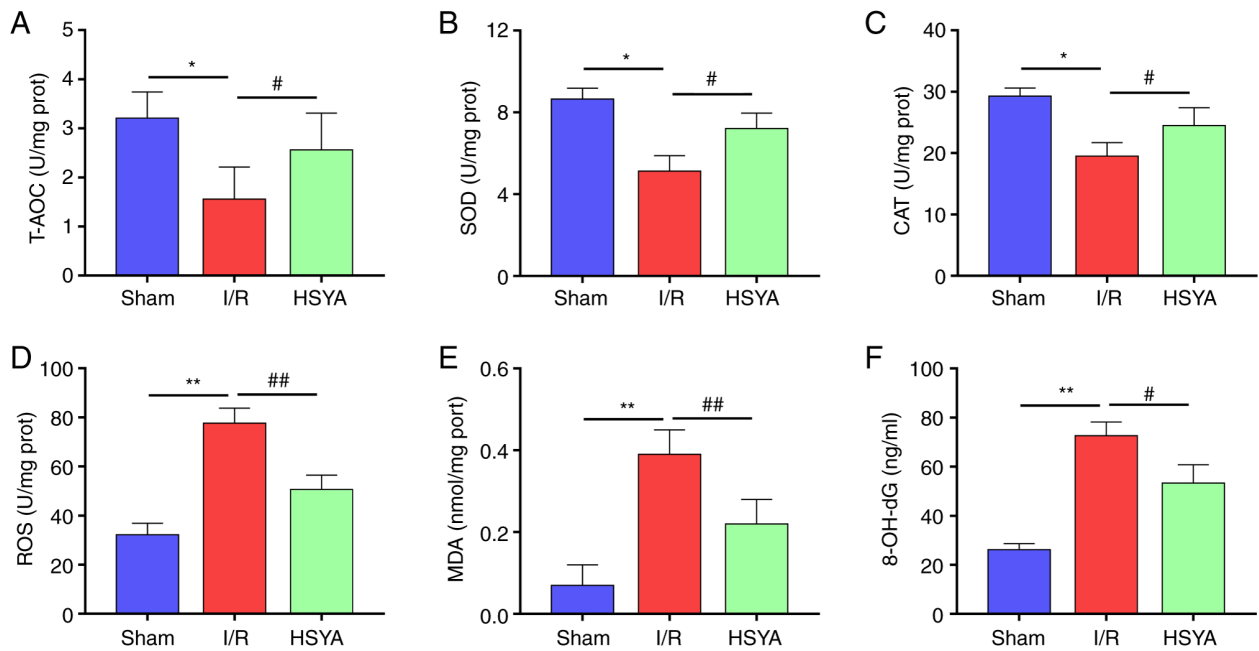


Figure 2. Effect of HSYA on oxidative stress and antioxidant biomarkers in the kidney of I/R mice. (A-C) The activities of (A) T-AOC, (B) SOD, and (C) CAT in the kidney tissue. (D-F) The levels of (D) ROS, (E) MDA, and (F) 8-OH-dG in the kidney tissue. All data are expressed as the mean \pm SD. $^{*}P<0.05$ and $^{**}P<0.01$, Sham group vs. I/R group; $^{##}P<0.01$ and $^{#}P<0.05$, I/R group vs. HSYA group. HSYA, Hydroxysafflor yellow A; I/R, ischemia/reperfusion; SOD, superoxide dismutase; CAT, catalase; ROS, reactive oxygen species; MDA, malondialdehyde; 8-OH-dG, 8-hydroxyguanosine.

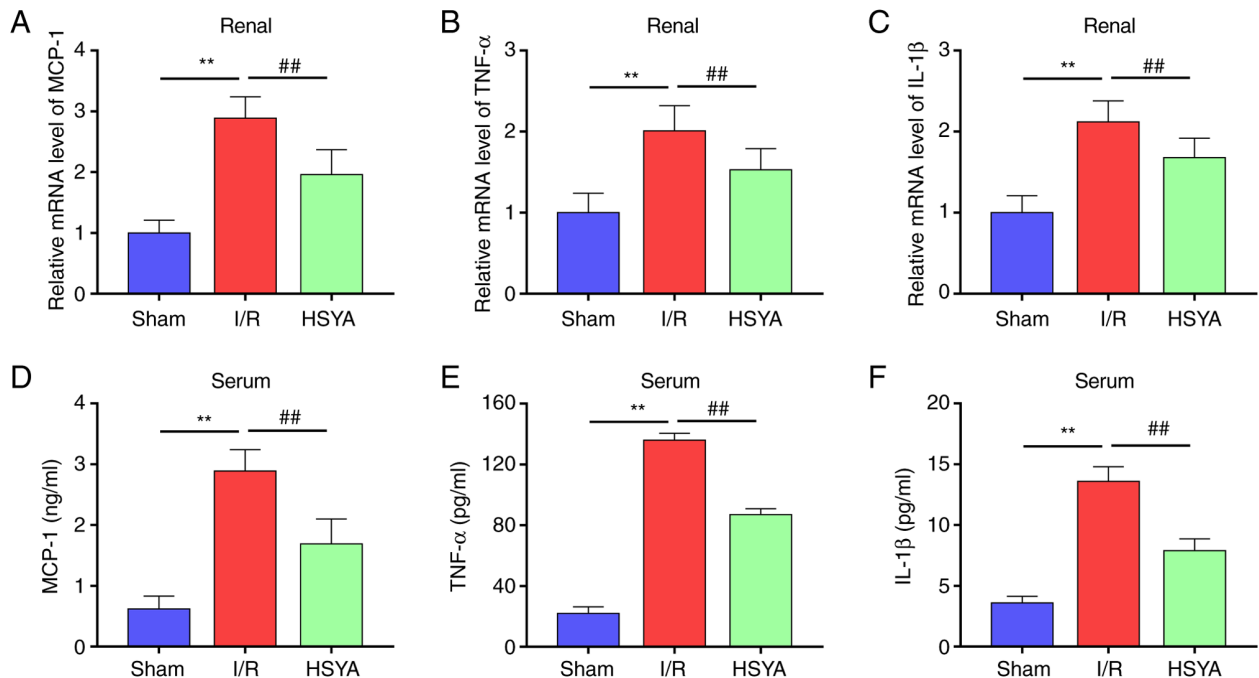


Figure 3. Effect of HSYA on proinflammatory cytokines in I/R mice. (A-C) The mRNA levels of (A) MCP-1, (B) TNF- α , and (C) IL-1 β in the kidney tissue. (D-F) The levels of (D) MCP-1, (E) TNF- α , and (F) IL-1 β in the serum. All data are expressed as the mean \pm SD. $^{**}P<0.01$, Sham group vs. I/R group; $^{##}P<0.01$, I/R group vs. HSYA group. HSYA, Hydroxysafflor yellow A; I/R, ischemia/reperfusion; MCP-1, monocyte chemoattractant protein-1; TNF- α , tumor necrosis factor- α ; IL-1 β , interleukin-1 β .

of proinflammatory cytokines in serum and kidney of I/R mice was further investigated. As revealed in Fig. 3, compared with the Sham group, the levels of MCP-1, TNF- α and IL-1 β significantly increased in the kidney and serum of I/R mice. Conversely, HSYA pretreatment significantly decreased the levels of MCP-1, TNF- α , and IL-1 β in the kidney and serum

of I/R mice. These results indicated that HSYA treatment suppresses the inflammatory response in I/R mice.

HSYA attenuates apoptosis in the kidney of I/R mice. To observe the cell apoptosis in the kidney of I/R mice, the expression of several apoptosis-associated proteins in the

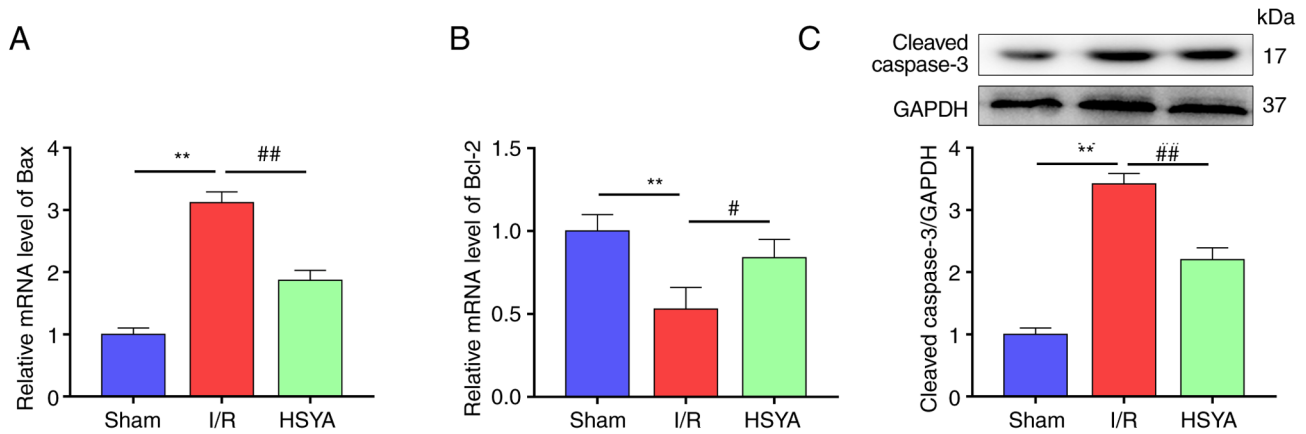


Figure 4. Effect of HSYA on cell apoptosis in the kidney of I/R mice. (A and B) The mRNA levels of (A) Bax and (B) Bcl-2 in the kidney tissue. (C) The expression of cleaved caspase-3 in the kidney tissue. All data are expressed as the mean \pm SD. ** $P < 0.01$, Sham group vs. I/R group; ## $P < 0.01$ and # $P < 0.05$, I/R group vs. HSYA group. HSYA, Hydroxysafflor yellow A; I/R, ischemia/reperfusion.

kidney was assessed. As demonstrated in Fig. 4A-C, compared with the Sham group, the levels of the pro-apoptotic proteins Bax and cleaved caspase-3 were significantly increased and the anti-apoptotic protein Bcl-2 was significantly decreased in the HSYA group. Conversely, HSYA pretreatment significantly attenuated the decrease of Bcl-2 and the increase of Bax and caspase-3 in comparison with the I/R group.

HSYA promotes the expression of the Akt/GSK-3 β /Fyn-Nrf2 axis in the kidney of I/R mice. Previous studies demonstrated that Nrf2 plays an important role in regulating inflammation and redox balance in the kidney (8-9,23). In the present study, it was found that the nuclear transfer of Nrf2 was significantly increased in mice with renal I/R compared with the Sham group (Fig. 5A and B). Accordingly, the expression of Nrf2 target antioxidant genes HO-1 and NQO1 were significantly higher in the I/R group compared with the Sham group (Fig. 5C-E). In addition, HSYA pretreatment further increased the nuclear transfer of Nrf2 and significantly improved the expression of Nrf2 target antioxidant genes HO-1 and NQO1 in comparison with the I/R group (Fig. 5A-E).

Previous studies indicated that the activation of Nrf2 is regulated by adjusting Fyn-mediated degradation and nuclear export of Nrf2 (24,25). To investigate the mechanisms by which HSYA treatment activates Nrf2 transcriptional functions in the kidney, the total and p-Akt, GSK-3 β , and nuclear Fyn levels were measured. As revealed in Fig. 5F-J, significantly increased phosphorylation of GSK-3 β and Akt and decreased nucleus Fyn level were identified in the I/R group compared with the Sham group. Furthermore, HSYA pretreatment further increased the phosphorylation of GSK-3 β and Akt and decreased the level of nucleus Fyn in comparison with the I/R group (Fig. 5F-J). These results suggested that HSYA attenuates renal damage in I/R mice by upregulating Akt/GSK-3 β /Fyn-Nrf2 axis-mediated antioxidant gene expression.

HSYA preserves the viability of H/R-treated HK-2 cells. Since HSYA pretreatment alleviated I/R kidney damage *in vivo*, the effect of HSYA on HK-2 cells was next investigated *in vitro* (Fig. 6A). As revealed in Fig. 6B, H/R significantly decreased

the viability of HK-2 cells, which was restored by HSYA treatment in a dose-dependent manner. Consistently, H/R significantly increased the levels of pro-apoptotic proteins Bax and cleaved caspase-3 and decreased the level of anti-apoptotic protein Bcl-2 in HK2 cells (Fig. 6C-E). Meanwhile, HSYA treatment alleviated the H/R-induced increase in Bax and cleaved caspase-3 expression and the decrease of Bcl-2 expression in HK2 cells (Fig. 6C-E). These results suggested that HSYA preserves the viability of H/R-treated HK-2 cells.

HSYA upregulates the antioxidant capacity and reduces the oxidative stress and inflammation of H/R-treated HK-2 cells. Furthermore, the effect of HSYA on the antioxidant capacity, oxidative stress, and inflammation of H/R-treated HK-2 cells was tested. As demonstrated in Fig. 7A-C, H/R significantly decreased the activities of T-AOC, SOD, and CAT of HK-2 cells. Furthermore, pretreatment with HSYA significantly increased the activities of T-AOC, SOD, and CAT of H/R-treated HK-2 cells.

On the other hand, H/R significantly increased the levels of oxidative stress biomarkers (ROS, MDA, and 8-OH-dG) and pro-inflammatory cytokines (MCP-1, TNF- α , and IL-1 β) of HK-2 cells (Fig. 7D-I). Conversely, HSYA pretreatment significantly decreased the levels of oxidative stress biomarkers and pro-inflammatory cytokines of H/R-treated HK-2 cells. Additionally, the effect of HSYA on the antioxidant capacity, oxidative stress, and inflammation of H/R-treated HK-2 cells showed a dose-dependent manner.

The Akt/GSK-3 β /Fyn-Nrf2 pathway is involved in the HSYA-mediated protective effect against H/R in HK-2 cells. It was further confirmed whether the Akt/GSK-3 β /Fyn-Nrf2 pathway was critical in the protective effects observed in H/R-treated HK-2 cells that were pretreated with HSYA. As shown in Fig. 8A-E, H/R significantly increased the nuclear transfer of Nrf2 and the expression of Nrf2 target antioxidant genes HO-1 and NQO1. HSYA pretreatment further increased the expression of these proteins in H/R-treated HK-2 cells. Moreover, significantly increased phosphorylation of Akt and GSK-3 β and decreased nucleus Fyn level was found in HK-2 cells (Fig. 8F-J). HSYA pretreatment significantly increased

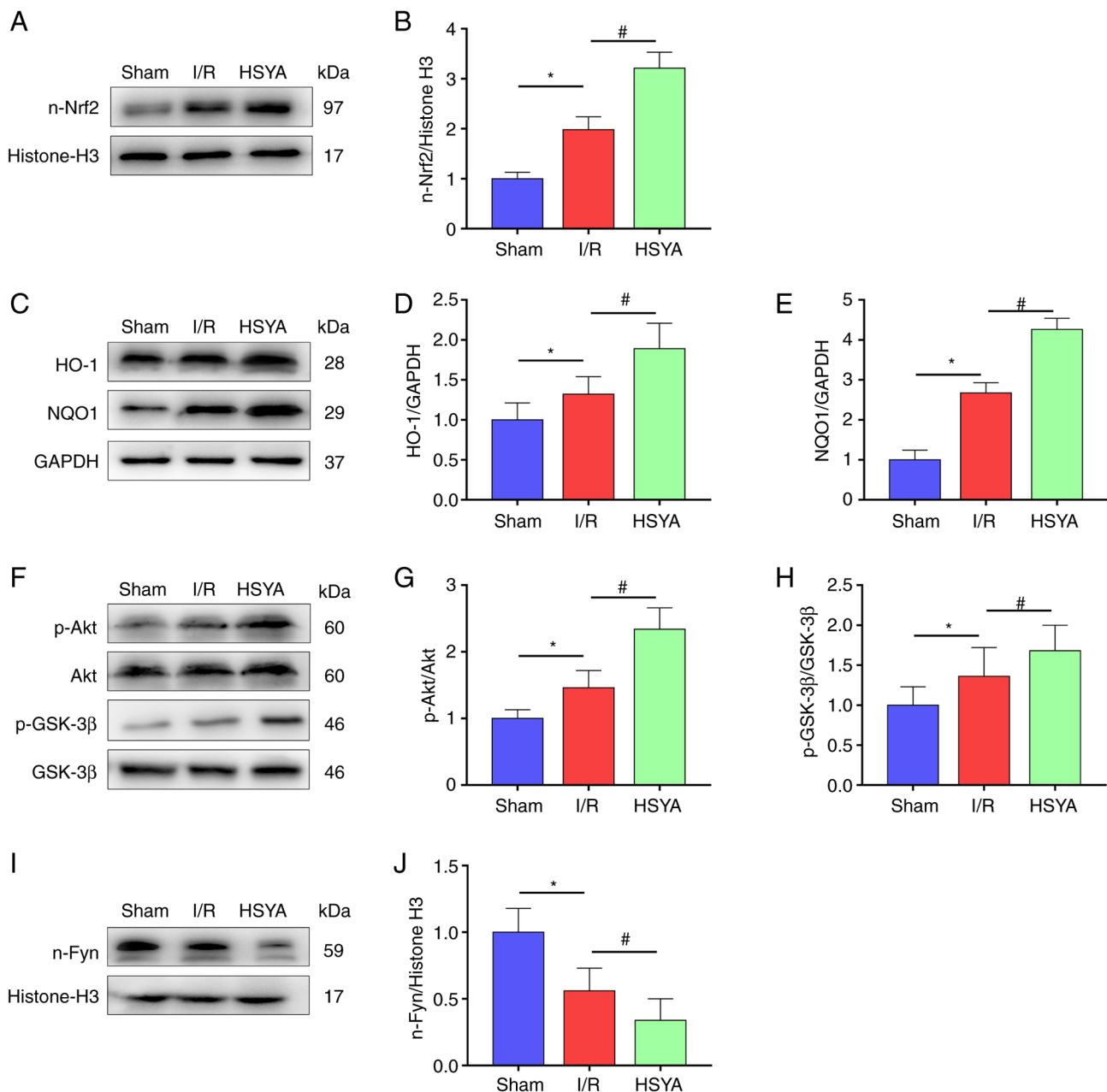


Figure 5. Effect of HSYA on the expression of the Akt/GSK-3 β /Fyn-Nrf2 axis in the kidney of I/R mice. (A and B) Representative western blot images and summarized data for the expression of nuclear Nrf2. (C-E) Representative western blot images and summarized data for the expression of (D) HO-1 and (E) NQO1. (F-H) Representative western blot images and summarized data for the ratio of (G) p-Akt/Akt and (H) p-GSK-3 β /GSK-3 β . (I and J) Representative western blot images and summarized data for the expression of nuclear Fyn. The following protein bands shown in this figure originated from the same gel/membrane: 1. HO-1, NQO1, and GAPDH; 2. n-Nrf2 and Histone-H3; 3. Akt, p-Akt, GSK-3 β , and p-GSK-3 β ; 4. n-Fyn and Histone-H3. All data are expressed as the mean \pm SD. * $P < 0.05$, Sham group vs. I/R group; # $P < 0.05$, I/R group vs. HSYA group. HSYA, Hydroxysafflor yellow A; I/R, ischemia/reperfusion; Nrf2, nuclear factor erythroid 2-related factor 2; HO-1, heme oxygenase-1; NQO1, NAD(P)H quinone oxidoreductase 1; p-, phosphorylated.

the phosphorylation of Akt and GSK-3 β and decreased nucleus Fyn level in H/R-treated HK-2 cells (Fig. 8F-J).

Subsequently, LY294002, an Akt inhibitor, was used to explore whether HSYA protected HK-2 cells by inhibiting the Akt/GSK-3 β /Fyn-Nrf2 pathway in the present study. As demonstrated in Fig. 8, significantly reduced nuclear Nrf2, HO-1, and NQO1 expression was observed in H/R-treated HK-2 cells after LY294002 supplementation. In addition, as demonstrated in Figs. 6 and 7, the HSYA-mediated improvement in antioxidant capacity and reduction in the expression of oxidative stress, pro-apoptotic, and pro-inflammatory

biomarkers in H/R-treated HK-2 cells were also abrogated by LY294002 supplementation. These data revealed that the protective effects of HSYA on H/R-treated HK-2 cells were dependent on the Akt/GSK-3 β /Fyn-Nrf2 pathway.

Discussion

It is well accepted that I/R-induced AKI is mainly characterized by oxidative stress, inflammation, and apoptosis, which results in higher rates of mortality and morbidity due to the lack of effective therapies (26). As the major active

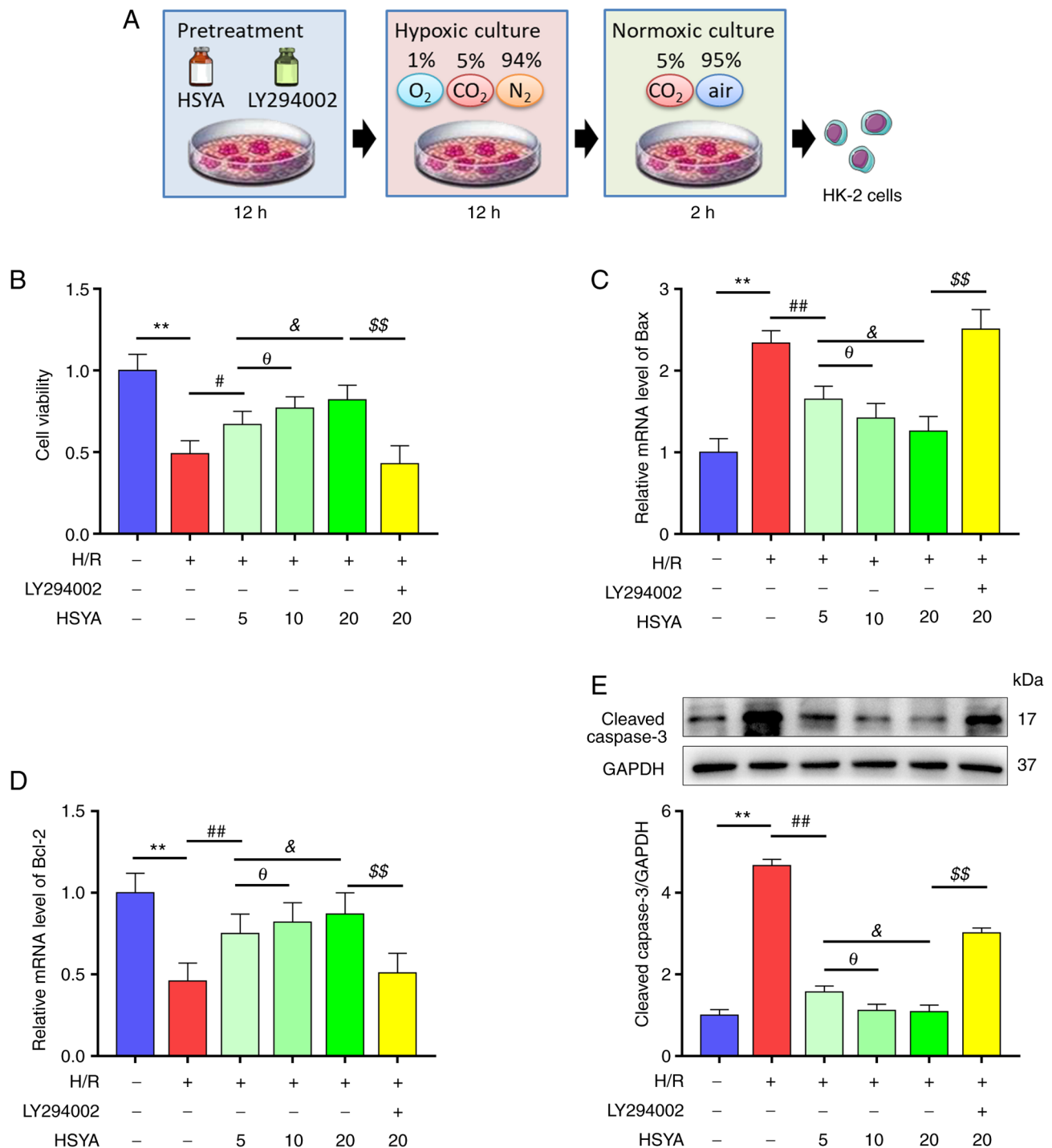


Figure 6. Effect of HSYA on the viability of H/R-treated HK-2 cells. HK-2 cells were pretreated with or without Akt inhibitor LY294002 (30 μ M) and HSYA at different doses (5, 10, 20 μ g/ml) for 12 h, and then were exposed to H/R. (A) The scheme of the H/R model. (B) Effects of HSYA on the cell viabilities of HK-2 cells. (C and D) Effects of HSYA on the mRNA levels of (C) Bax and (D) Bcl-2 in HK-2 cells. (E) Effects of HSYA on the expression of cleaved caspase-3 in HK-2 cells. All data are expressed as the mean \pm SD. ** P <0.01, control group vs. H/R group; ## P <0.01 and * P <0.05, H/R group vs. 5 μ g/ml HSYA group; θ P <0.05, 5 μ g/ml HSYA group vs. 10 μ g/ml HSYA group; & P <0.05, 5 μ g/ml HSYA group vs. 20 μ g/ml HSYA group; \$\$ P <0.01, 20 μ g/ml HSYA group vs. LY294002 group. This image was produced using images from Servier Medical Art, licensed under a Creative Common Attribution 3.0 Generic License <http://smart.servier.com>. HSYA, Hydroxysafflor yellow A; H/R, hypoxia/reoxygenation.

component of *C. tinctorius* L., HSYA has been studied for the treatment of AKI and presents positive therapeutic roles (15). The potential molecular mechanism of HSYA's therapeutic effect was explored from a new perspective of regulating the Nrf2 antioxidant signal axis and affecting the redox metabolism of renal tissue. In the present study,

it was demonstrated that pretreatment with HSYA could significantly attenuate the imbalance of redox metabolism, inflammatory responses, and apoptosis in renal I/R injury by targeting the Akt/GSK-3 β /Fyn-Nrf2 axis. These findings uncovered certain novel molecular events in HSYA that protect I/R-induced AKI.

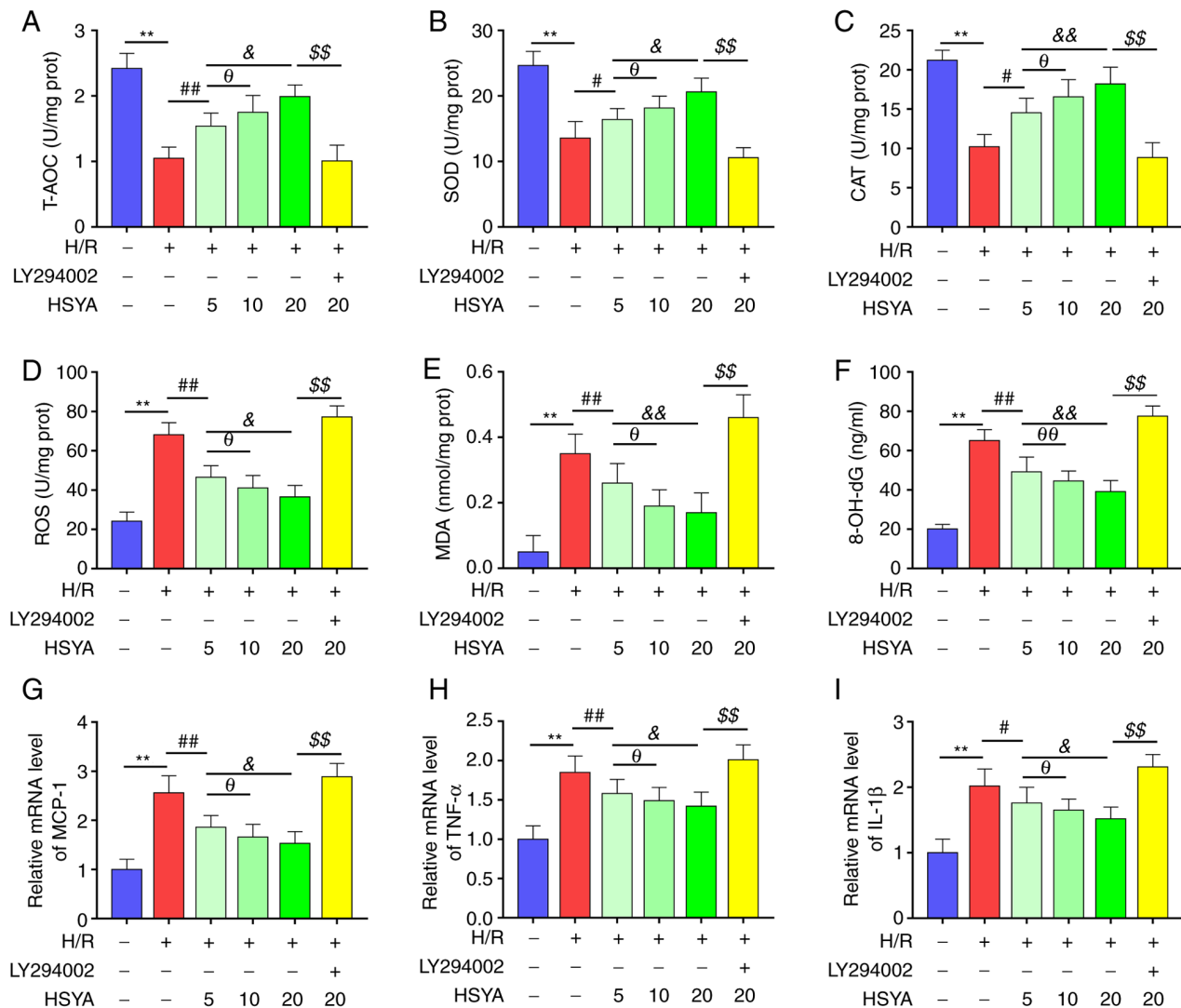


Figure 7. Effect of HSYA on the antioxidant capacity, oxidative stress, and inflammation of H/R-treated HK-2 cells. The activities of T-AOC (A), SOD (B), and CAT (C) in HK-2 cells. The levels of ROS (D), MDA (E), and 8-OH-dG (F) in HK-2 cells. The mRNA levels of MCP-1 (G), TNF- α (H), and IL-1 β (I) in HK-2 cells. All data are expressed as the mean \pm SD. ** P <0.01, control group vs. H/R group; ## P <0.01, P <0.05, H/R group vs. 5 μ g/ml HSYA group; # P <0.05, 5 μ g/ml HSYA group vs. 10 μ g/ml HSYA group; &# P <0.01, &# P <0.05, 5 μ g/ml HSYA group vs. 20 μ g/ml HSYA group; \$\$\$ P <0.01, 20 μ g/ml HSYA group vs. LY294002 group. HSYA, Hydroxysafflor yellow A; H/R, hypoxia/reoxygenation; SOD, superoxide dismutase; CAT, catalase; ROS, reactive oxygen species; MDA, malondialdehyde; 8-OH-dG, 8-hydroxyguanosine.

Accumulating evidence has suggested that oxidative stress and inflammation play a critical role in the pathology of I/R injury (27,28). In the present study, significantly raised oxidative stress biomarkers (ROS, MDA, and 8-OH-dG) and pro-inflammatory cytokines (MCP-1, TNF- α , and IL-1 β), and decreased antioxidant enzyme activities of T-AOC, SOD, and CAT were also observed in I/R mice. Meanwhile, I/R resulted in renal dysfunction and pathological damage. Consistent with previous studies (15,29), it was found that HSYA treatment ameliorated renal damage and dysfunction in I/R mice. It has been evidenced that endogenous inflammatory mediators enhance the renal injury, dysfunction, and inflammation caused by I/R (30,31). Previous studies demonstrated that HSYA protected against kidney injury, which may be related to its anti-inflammatory action (32-35). Similarly, it was identified that HSYA treatment significantly decreased the levels of pro-inflammatory cytokines MCP-1, TNF- α , and IL-1 β in I/R mice and H/R-treated HK-2 cells. Recently, Lee *et al* (36) identified that the activity

of SOD was markedly increased and the level of MDA was markedly decreased in HSYA-treated diabetic nephropathy rats. Wei *et al* (37) also found that HSYA treatment significantly attenuated the elevation of MDA content, the decrease in SOD activity, and the T-AOC in I/R-induced brain injury. MDA and 8-OH-dG are end-products of ROS-induced lipid peroxidation and DNA oxidation that are commonly used as oxidative stress biomarkers (6). In the present study, it was reported that HSYA treatment significantly upregulated the activities of T-AOC, SOD, and CAT, while significantly downregulated the levels of ROS, MDA, and 8-OH-dG both *in vivo* and *in vitro*. These results indicated that HSYA treatment alleviates the imbalance of redox metabolic and inflammatory response induced by kidney I/R injury.

It has been reported that I/R can induce apoptosis of numerous tissues and organs with the activation of a series of apoptotic pathways (38,39). Previous studies have demonstrated that the ratio of pro-apoptotic protein Bax

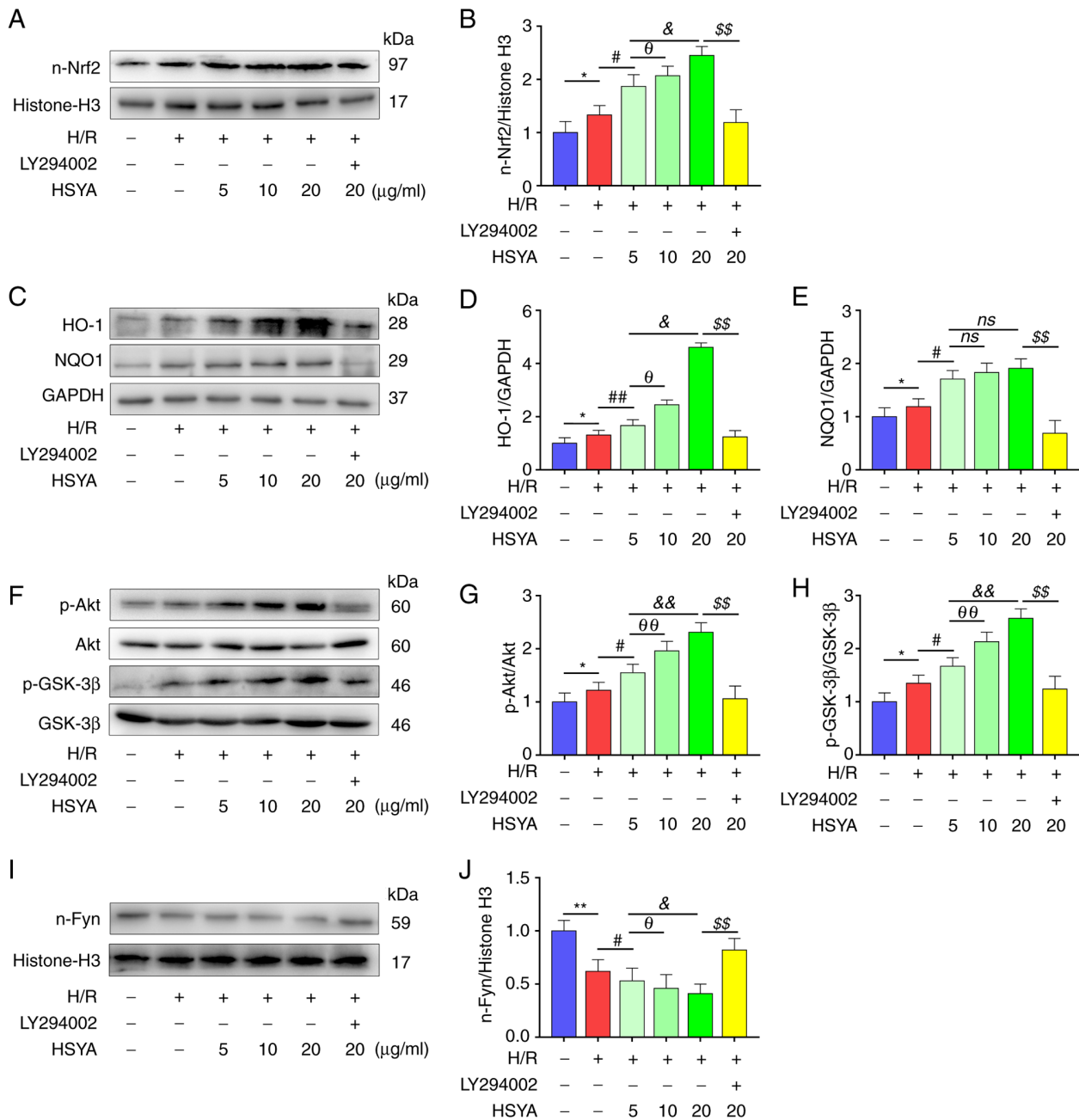


Figure 8. Effect of HSYA on the expression of the Akt/GSK-3 β /Fyn-Nrf2 axis of H/R-treated HK-2 cells. (A and B) Representative western blot images and summarized data for the expression of nuclear Nrf2. (C-E) Representative western blot images and summarized data for the expression of (D) HO-1 and (E) NQO1. (F-H) Representative western blot images and summarized data for the ratio of (G) p-Akt/Akt and (H) p-GSK-3 β /GSK-3 β . (I and J) Representative western blot images and summarized data for the expression of nuclear Fyn. The following groups protein bands shown in this figure originated from the same gel/membrane: 1. HO-1, NQO1, and GAPDH; 2. n-Nrf2 and Histone-H3; 3. Akt, p-Akt, GSK-3 β , and p-GSK-3 β ; 4. n-Fyn and Histone-H3. All data are expressed as the mean \pm SD. ** P <0.01 and * P <0.05, control group vs. H/R group; ## P <0.01 and # P <0.05, H/R group vs. 5 μ g/ml HSYA group; $^{\theta}$ P <0.01 and $^{\theta}$ P <0.05, 5 μ g/ml HSYA group vs. 10 μ g/ml HSYA group; && P <0.01 and & P <0.05, 5 μ g/ml HSYA group vs. 20 μ g/ml HSYA group; \$\$ P <0.01, 20 μ g/ml HSYA group vs. LY294002 group. HSYA, Hydroxysafflor yellow A; H/R, hypoxia/reoxygenation; Nrf2, nuclear factor erythroid 2-related factor 2; HO-1, heme oxygenase-1; NQO1, NAD(P)H quinone oxidoreductase 1; p-, phosphorylated.

to anti-apoptotic protein Bcl-2 was an important element in determining the threshold of apoptosis (40). In the present study, it was revealed that HSYA treatment markedly restores the upregulation of Bax and the downregulation of Bcl-2 in kidney cells induced by *in vivo* I/R or *in vitro* H/R. The family of caspases are crucial executors of programmed apoptosis. Among them, caspase-3 has been found to be processed into activated fragments such as cleaved caspase-3 when activated by the apoptotic pathway, which is considered as an index of

apoptosis (41). In the present study, it was revealed that HSYA treatment significantly reduces the level of cleaved caspase-3 in kidney cells both *in vivo* and *in vitro*. These data suggested that HSYA intervention can alleviate I/R-induced renal injury by exerting an anti-apoptotic effect.

Furthermore, the potential molecular mechanisms related to the protective roles of HSYA against renal I/R injury were also examined. The Nrf2 pathway regulates the expression of several antioxidant and detoxification enzymes including

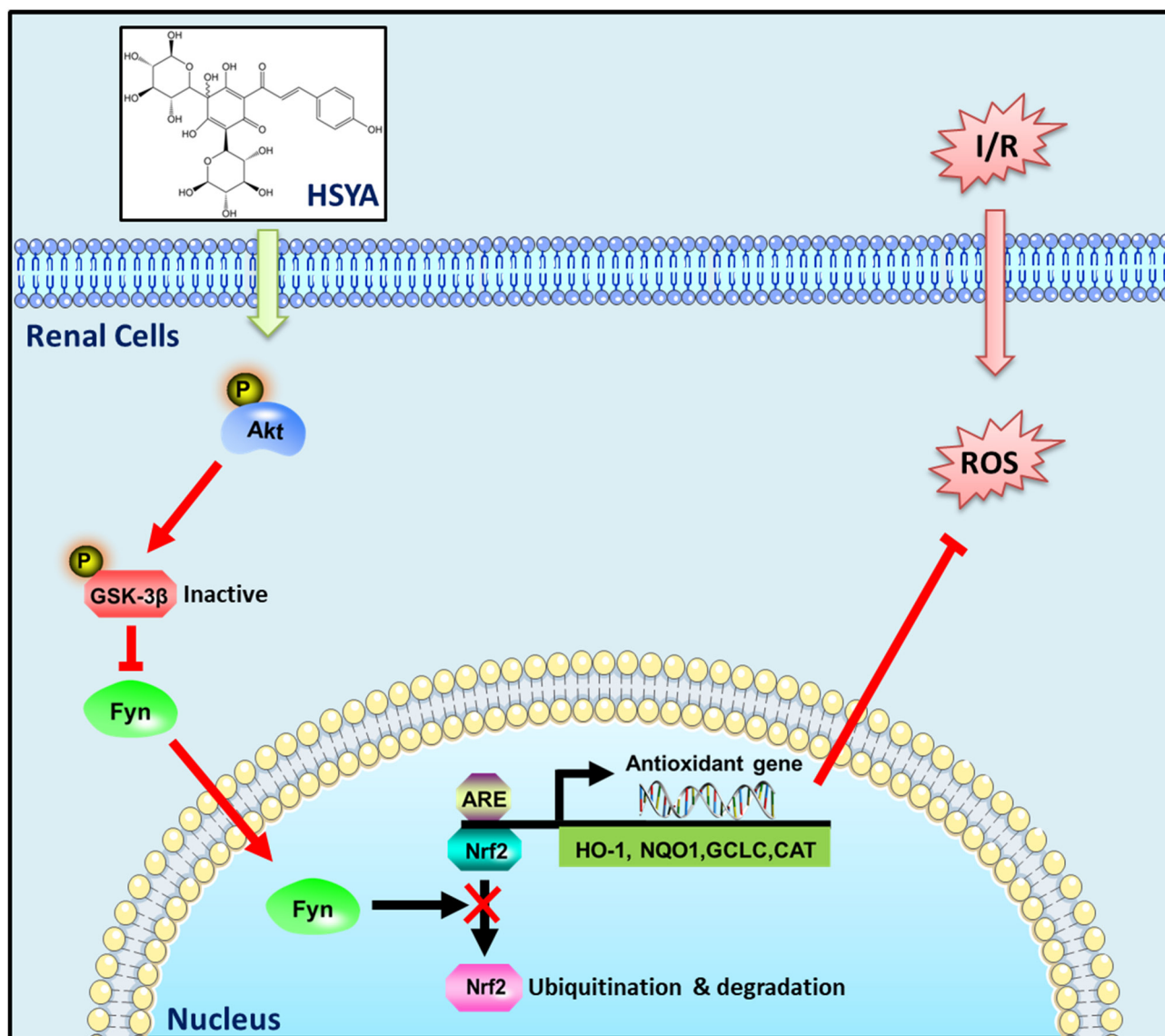


Figure 9. Schematic illustration of the protective effects of HSYA on I/R-induced kidney injury by targeting the Akt/GSK-3 β /Fyn-Nrf2 axis. This image was produced using images from Servier Medical Art, licensed under a Creative Common Attribution 3.0 Generic License <http://smart.servier.com>. HSYA, Hydroxysafflor yellow A; H/R, hypoxia/reoxygenation; I/R, ischemia/reperfusion; ROS, reactive oxygen species; Nrf2, nuclear factor erythroid 2-related factor 2.

the catalytic subunits of glutamate cysteine ligase, heme oxygenase-1 (HO-1), and NAD(P)H quinone oxidoreductase 1 (NQO1) by binding to the antioxidant response element in their promoter regions (6,42-44). A previous study suggested that HSYA can improve the antioxidant capacity of target organs by activating Nrf2 pathway and alleviate tissue injury induced by I/R (16). Ni *et al* found that activation of the AMPK/Nrf-2/HO-1 pathway can inhibit the inflammatory response of lipopolysaccharide-induced acute lung injury (45). El-Emam *et al* identified that activation of the Nrf-2/HO-1 pathway plays an anti-apoptotic effect in hepatic I/R injury (46). Previous studies have shown that although the total Nrf2 expression level (or the Nrf2 nuclear/cytosolic ratio) could change under different physiological and pathological conditions, the impact on the regulation of downstream antioxidant gene expression remains highly dependent on the Nrf2 level that is transported into the nucleus after activation (24,47,48).

In the present study, it was observed that HSYA treatment significantly increased the nuclear transfer of Nrf2 and improved the expression of its downstream target genes HO-1 and NQO1 in comparison with the I/R group. Both literature studies and the current research suggested that the activation of Nrf2 was regulated by Akt/GSK-3 β /Fyn-mediated degradation and nuclear export of Nrf2 (24,43,49). In the present study, the significantly increased phosphorylation of GSK-3 β and Akt and decreased nucleus Fyn level in the HSYA treatment group compared with the I/R group were also demonstrated. *In vitro*, it was revealed that the intervention of Akt inhibitor LY294002 significantly reduced nuclear Nrf2, HO-1, and NQO1 expression in H/R-treated HK-2 cells. In addition, HSYA-mediated improvement in antioxidant, anti-inflammatory, and anti-apoptotic effects in H/R-treated HK-2 cells was also abrogated by LY294002 supplementation. Collectively, these results provided important insights

into the protective effects of HSYA on I/R- or H/R-induced renal cells injury were dependent on the activation of Akt/GSK-3 β /Fyn-Nrf2 axis.

It should be pointed out that although the *in vitro* H/R model is commonly used to simulate I/R injury *in vivo*, it is still unable to accurately replicate the complex internal environment, such as changes in inflammatory conditions (50,51). In addition, although the present study showed that HSYA can alleviate renal tubular injury caused by I/R, it has been claimed that I/R also causes pathological damage to other components of the kidney. For instance, glomerular pathological damage that manifests as glomerular hyperplasia, hypertrophy, mesangial cell hyperplasia, anomalies in the basement membrane, and inflammatory cell infiltration is also present in I/R renal injury (52,53). Consequently, the repair effect and molecular mechanism of HSYA on these I/R injured kidney tissues need to be further clarified.

In summary, the results of the present study revealed that HSYA exerts antioxidant, anti-inflammatory, and anti-apoptotic effects against AKI induced by I/R, at least in part, via targeting the Akt/GSK-3 β /Fyn-Nrf2 axis (Fig. 9). Our studies present a promising use for HSYA in the treatment of renal I/R injury.

Acknowledgements

Not applicable.

Funding

The present study was supported by the National Natural Science Foundation of China (grant nos. 32200731 and 32070781), the Shandong Provincial Natural Science Foundation (grant nos. ZR2021MC064 and ZR2020MH166) and the Shandong Province Traditional Chinese Medicine Science and Technology Project (grant no. 2020Q061).

Availability of data and materials

The datasets used and/or analyzed during the current study are available from the corresponding author on reasonable request.

Authors' contributions

YW, YX and XL conceived and designed the experiments. ZG, JK, KH, ZL and XT performed the experiments. CW, HZ and YZ analyzed the data. YX wrote the paper. YW and YX confirm the authenticity of all the raw data. All authors read and approved the final manuscript.

Ethics approval and consent to participate

The present study protocol was reviewed and approved (approval no. 2021-11) by the Ethics Committee of Binzhou Medical University (Yantai, China).

Patient consent for publication

Not applicable.

Competing interests

The authors declare that they have no competing interests.

References

1. Bao N and Dai D: Dexmedetomidine protects against ischemia and reperfusion-induced kidney injury in rats. *Mediators Inflamm* 2020: 2120971, 2020.
2. Malek M and Nematbakhsh M: Renal ischemia/reperfusion injury; from pathophysiology to treatment. *J Renal Inj Prev* 4: 20-27, 2015.
3. Diao C, Chen Z, Qiu T, Liu H, Yang Y, Liu X, Wu J and Wang L: Inhibition of PRMT5 attenuates oxidative stress-induced pyroptosis via activation of the Nrf2/HO-1 signal pathway in a mouse model of renal ischemia-reperfusion injury. *Oxid Med Cell Longev* 2019: 2345658, 2019.
4. Liu H, Wang L, Weng X, Chen H, Du Y, Diao C, Chen Z and Liu X: Inhibition of Brd4 alleviates renal ischemia/reperfusion injury-induced apoptosis and endoplasmic reticulum stress by blocking FoxO4-mediated oxidative stress. *Redox Biol* 24: 101195, 2019.
5. Tang C, Han H, Liu Z, Liu Y, Yin L, Cai J, He L, Liu Y, Chen G, Zhang Z, *et al*: Activation of BNIP3-mediated mitophagy protects against renal ischemia-reperfusion injury. *Cell Death Dis* 10: 677, 2019.
6. Wang Y, Xiong Y, Zhang A, Zhao N, Zhang J, Zhao D, Yu Z, Xu N, Yin Y, Luan X and Xiong Y: Oligosaccharide attenuates aging-related liver dysfunction by activating Nrf2 antioxidant signaling. *Food Sci Nutr* 8: 3872-3881, 2020.
7. Jiang GP, Liao YJ, Huang LL, Zeng XJ and Liao XH: Effects and molecular mechanism of pachymic acid on ferroptosis in renal ischemia reperfusion injury. *Mol Med Rep* 23: 63, 2021.
8. Sun Q, Zeng C, Du L and Dong C: Mechanism of circadian regulation of the NRF2/ARE pathway in renal ischemia-reperfusion. *Exp Ther Med* 21: 190, 2021.
9. Pei J, Cai S, Song S, Xu Y, Feng M, Luo G, Wang Y, Sun F, Shi H and Xu S: Normobaric hyperoxia plays a protective role against renal ischemia-reperfusion injury by activating the Nrf2/HO-1 signaling pathway. *Biochem Biophys Res Commun* 532: 151-158, 2020.
10. Hu ZC, Xie ZJ, Tang Q, Li XB, Fu X, Feng ZH, Xuan JW, Ni WF and Wu AM: Hydroxysafflor yellow A (HSYA) targets the NF- κ B and MAPK pathways and ameliorates the development of osteoarthritis. *Food Funct* 9: 4443-4456, 2018.
11. Chen L, Xiang Y, Kong L, Zhang X, Sun B, Wei X and Liu H: Hydroxysafflor yellow A protects against cerebral ischemia-reperfusion injury by anti-apoptotic effect through PI3K/Akt/GSK3 β pathway in rat. *Neurochem Res* 38: 2268-2275, 2013.
12. Zhou D, Ding T, Ni B, Jing Y and Liu S: Hydroxysafflor Yellow A mitigated myocardial ischemia/reperfusion injury by inhibiting the activation of the JAK2/STAT1 pathway. *Int J Mol Med* 44: 405-416, 2019.
13. Ye J, Lu S, Wang M, Ge W, Liu H, Qi Y, Fu J, Zhang Q, Zhang B, Sun G and Sun X: Hydroxysafflor yellow A protects against myocardial ischemia/reperfusion injury via suppressing NLRP3 inflammasome and activating autophagy. *Front Pharmacol* 11: 1170, 2020.
14. Jiang S, Shi Z, Li C, Ma C, Bai X and Wang C: Hydroxysafflor yellow A attenuates ischemia/reperfusion-induced liver injury by suppressing macrophage activation. *Int J Clin Exp Pathol* 7: 2595-2608, 2014.
15. Bai J, Zhao J, Cui D, Wang F, Song Y, Cheng L, Gao K, Wang J, Li L, Li S, *et al*: Protective effect of hydroxysafflor yellow A against acute kidney injury via the TLR4/NF- κ B signaling pathway. *Sci Rep* 8: 9173, 2018.
16. Hu T, Wei G, Xi M, Yan J, Wu X, Wang Y, Zhu Y, Wang C and Wen A: Synergistic cardioprotective effects of Danshensu and hydroxysafflor yellow A against myocardial ischemia-reperfusion injury are mediated through the Akt/Nrf2/HO-1 pathway. *Int J Mol Med* 38: 83-94, 2016.
17. Yakulov TA, Todkar AP, Slanchev K, Wiegel J, Bona A, Groß M, Scholz A, Hess I, Wurditsch A, Grahmmer F, *et al*: CXCL12 and MYC control energy metabolism to support adaptive responses after kidney injury. *Nat Commun* 9: 3660, 2018.
18. Brooks C, Wei Q, Cho SG and Dong Z: Regulation of mitochondrial dynamics in acute kidney injury in cell culture and rodent models. *J Clin Invest* 119: 1275-1285, 2009.

19. Livak KJ and Schmittgen TD: Analysis of relative gene expression data using real-time quantitative PCR and the 2(-Delta Delta C(T)) method. *Methods* 25: 402-408, 2001.
20. Wang Y, Zhao N, Xiong Y, Zhang J, Zhao D, Yin Y, Song L, Yin Y, Wang J, Luan X and Xiong Y: Downregulated recycling process but not de novo synthesis of glutathione limits antioxidant capacity of erythrocytes in hypoxia. *Oxid Med Cell Longev* 2020: 7834252, 2020.
21. Yu W, Sheng M, Xu R, Yu J, Cui K, Tong J, Shi L, Ren H and Du H: Berberine protects human renal proximal tubular cells from hypoxia/reoxygenation injury via inhibiting endoplasmic reticulum and mitochondrial stress pathways. *J Transl Med* 11: 24, 2013.
22. Liu C, Chen K, Wang H, Zhang Y, Duan X, Xue Y, He H, Huang Y, Chen Z, Ren H, *et al*: Gastrin attenuates renal ischemia/reperfusion injury by a PI3K/Akt/bad-mediated anti-apoptosis signaling. *Front Pharmacol* 11: 540479, 2020.
23. Nezu M and Suzuki N: Roles of Nrf2 in protecting the kidney from oxidative damage. *Int J Mol Sci* 21: 2951, 2020.
24. Dai X, Yan X, Zeng J, Chen J, Wang Y, Chen J, Li Y, Barati MT, Wintergerst KA, Pan K, *et al*: Elevating CXCR7 improves angiogenic function of EPCs via Akt/GSK-3 β /Fyn-mediated Nrf2 activation in diabetic limb ischemia. *Circ Res* 120: e7-e23, 2017.
25. Rong H, Liang Y and Niu Y: Rosmarinic acid attenuates β -amyloid-induced oxidative stress via Akt/GSK-3 β /Fyn-mediated Nrf2 activation in PC12 cells. *Free Radic Biol Med* 120: 114-123, 2018.
26. Borthwick E and Ferguson A: Perioperative acute kidney injury: Risk factors, recognition, management, and outcomes. *BMJ* 341: c3365, 2010.
27. Wu MY, Yang GT, Liao WT, Tsai A, Cheng YL, Cheng PW, Li CY and Li CJ: Current mechanistic concepts in ischemia and reperfusion injury. *Cell Physiol Biochem* 46: 1650-1667, 2018.
28. Amirzargar MA, Yaghubi F, Hosseiniapanah M, Jafari M, Pourjafar M, Rezaeipoor M, Rezaei H, Roshanaei G, Hajilooi M and Solgi G: Anti-inflammatory effects of valproic acid in a rat model of renal ischemia/reperfusion injury: Alteration in cytokine profile. *Inflammation* 40: 1310-1318, 2017.
29. Min J and Wei C: Hydroxysafflor yellow A cardioprotection in ischemia-reperfusion (I/R) injury mainly via Akt/hexokinase II independent of ERK/GSK-3 β pathway. *Biomed Pharmacother* 87: 419-426, 2017.
30. Ramesh G and Reeves WB: TNF- α mediates chemokine and cytokine expression and renal injury in cisplatin nephrotoxicity. *J Clin Invest* 110: 835-842, 2002.
31. Patel NS, Chatterjee PK, Di Paola R, Mazzon E, Britti D, De Sarro A, Cuzzocrea S and Thiemermann C: Endogenous interleukin-6 enhances the renal injury, dysfunction, and inflammation caused by ischemia/reperfusion. *J Pharmacol Exp Ther* 312: 1170-1178, 2005.
32. Ye J, Lu S, Wang M, Ge W, Liu H, Qi Y, Fu J, Zhang Q, Zhang B, Sun G and Sun X: Corrigendum: Hydroxysafflor yellow A protects against myocardial ischemia/reperfusion injury via suppressing NLRP3 inflammasome and activating autophagy. *Front Pharmacol* 12: 671318, 2021.
33. Hu N, Duan J, Li H, Wang Y, Wang F, Chu J, Sun J, Liu M, Wang C, Lu C and Wen A: Hydroxysafflor yellow A ameliorates renal fibrosis by suppressing TGF- β 1-induced epithelial-to-mesenchymal transition. *PLoS One* 11: e0153409, 2016.
34. Li J, Zhang S, Lu M, Chen Z, Chen C, Han L, Zhang M and Xu Y: Hydroxysafflor yellow A suppresses inflammatory responses of BV2 microglia after oxygen-glucose deprivation. *Neurosci Lett* 535: 51-56, 2013.
35. Liu S, Wang Y, Wen H, Sun X and Wang Y: Hydroxysafflor Yellow A inhibits TNF- α -induced inflammation of human fetal lung fibroblasts via NF- κ B signaling pathway. *Evid Based Complement Alternat Med* 2019: 4050327, 2019.
36. Lee M, Zhao H, Liu X, Liu D, Chen J, Li Z, Chu S, Kou X, Liao S, Deng Y, *et al*: Protective effect of hydroxysafflor yellow A on nephropathy by attenuating oxidative stress and inhibiting apoptosis in induced type 2 diabetes in rat. *Oxid Med Cell Longev* 2020: 7805393, 2020.
37. Wei X, Liu H, Sun X, Fu F, Zhang X, Wang J, An J and Ding H: Hydroxysafflor yellow A protects rat brains against ischemia-reperfusion injury by antioxidant action. *Neurosci Lett* 386: 58-62, 2005.
38. Yao L, Chen H, Wu Q and Xie K: Hydrogen-rich saline alleviates inflammation and apoptosis in myocardial I/R injury via PINK-mediated autophagy. *Int J Mol Med* 44: 1048-1062, 2019.
39. Ye L, He S, Mao X, Zhang Y, Cai Y and Li S: Effect of hepatic macrophage polarization and apoptosis on liver ischemia and reperfusion injury during liver transplantation. *Front Immunol* 11: 1193, 2020.
40. Yang E, Zha J, Jockel J, Boise LH, Thompson CB and Korsmeyer SJ: Bad, a heterodimeric partner for Bcl-XL and Bcl-2, displaces Bax and promotes cell death. *Cell* 80: 285-291, 1995.
41. Liang Y, Yan C and Schor NF: Apoptosis in the absence of caspase 3. *Oncogene* 20: 6570-6578, 2001.
42. Kubben N, Zhang W, Wang L, Voss TC, Yang J, Qu J, Liu GH and Misteli T: Repression of the antioxidant NRF2 pathway in premature aging. *Cell* 165: 1361-1374, 2016.
43. Xiong Y, Wang Y, Zhang J, Zhao N, Zhang H, Zhang A, Zhao D, Yu Z, Yin Y, Song L, *et al*: hPMSCs protects against D-galactose-induced oxidative damage of CD4(+) T cells through activating Akt-mediated Nrf2 antioxidant signaling. *Stem Cell Res Ther* 11: 468, 2020.
44. Xiong Y, Xiong Y, Zhang H, Zhao Y, Han K, Zhang J, Zhao D, Yu Z, Geng Z, Wang L, *et al*: hPMSCs-derived exosomal miRNA-21 protects against aging-related oxidative damage of CD4(+) T cells by targeting the PTEN/PI3K-Nrf2 axis. *Front Immunol* 12: 780897, 2021.
45. Ni YL, Shen HT, Su CH, Chen WY, Huang-Liu R, Chen CJ, Chen SP and Kuan YH: Nerolidol suppresses the inflammatory response during lipopolysaccharide-induced acute lung injury via the modulation of antioxidant enzymes and the AMPK/Nrf-2/HO-1 pathway. *Oxid Med Cell Longev* 2019: 9605980, 2019.
46. El-Emam SZ, Soubh AA, Al-Mokaddem AK and Abo El-Ella DM: Geraniol activates Nrf-2/HO-1 signaling pathway mediating protection against oxidative stress-induced apoptosis in hepatic ischemia-reperfusion injury. *Naunyn Schmiedeberg Arch Pharmacol* 393: 1849-1858, 2020.
47. Jain AK and Jaiswal AK: GSK-3 β acts upstream of Fyn kinase in regulation of nuclear export and degradation of NF-E2 related factor 2. *J Biol Chem* 282: 16502-16510, 2007.
48. Kaspar JW and Jaiswal AK: Tyrosine phosphorylation controls nuclear export of Fyn, allowing Nrf2 activation of cytoprotective gene expression. *FASEB J* 25: 1076-1087, 2011.
49. Zhao Y, Song W, Wang Z, Wang Z, Jin X, Xu J, Bai L, Li Y, Cui J and Cai L: Resveratrol attenuates testicular apoptosis in type 1 diabetic mice: Role of Akt-mediated Nrf2 activation and p62-dependent Keap1 degradation. *Redox Biol* 14: 609-617, 2018.
50. Ding C, Ding X, Zheng J, Wang B, Li Y, Xiang H, Dou M, Qiao Y, Tian P and Xue W: miR-182-5p and miR-378a-3p regulate ferroptosis in I/R-induced renal injury. *Cell Death Dis* 11: 929, 2020.
51. Dong Y, Yin J, Chen T, Wen J, Zhang Q, Li X, Lin W, Liu F, Fan Y and Wang N: DL-3-n-butylphthalide pretreatment attenuates renal ischemia/reperfusion injury. *Biochem Biophys Res Commun* 557: 166-173, 2021.
52. Golmohammadi MG, Banaei S, Nejati K and Chinifroush-Asl MM: Vitamin D3 and erythropoietin protect against renal ischemia-reperfusion injury via heat shock protein 70 and microRNA-21 expression. *Sci Rep* 10: 20906, 2020.
53. Chen Y, Lin L, Tao X, Song Y, Cui J and Wan J: The role of podocyte damage in the etiology of ischemia-reperfusion acute kidney injury and post-injury fibrosis. *BMC Nephrol* 20: 106, 2019.



This work is licensed under a Creative Commons Attribution-NonCommercial-NoDerivatives 4.0 International (CC BY-NC-ND 4.0) License.